Intramolecular Electron Transfer between Noncovalently Linked Donor and Acceptor in a [2]Catenane

Yi-Zhen Hu,[1] Dietmar van Loyen,[1] Oliver Schwarz,[1] Stefan Bossmann,[2] Heinz Dürr,*[,1] Volker Huch,[3] and Michael Veith[3]

FR 11.2 Organische Chemie and FR 11.1 Anorganische Chemie Universität des Saarlandes, Im Stadtwald 66041 Saarbrücken, Germany
Engler-Bunte Institut der Universität Karlsruhe 76128, Karlsruhe, Germany

Received January 29, 1998

The photosynthetic reaction center represents an evolutionary optimized organized assembly where vectorial photoinduced electron transfer leads to effective charge separation.[4] Many of the more hotly debated issues in the biological electron-transfer (ET) systems involve questions of how electron-transfer events proceed through noncovalently linked protein pathways.[5] Substantial efforts were directed to prepare noncovalently linked photosynthetic model systems that might allow for the study of ET processes in formally unlinked but still well-associated donor−acceptor aggregates.[6] With regard to the design of model systems for the photosynthetic reaction center, many transition-metal complexes including rotaxanes and catenanes have been investigated during the past few years.[7] In our group, many supramolecular components have been prepared and characterized.[8a−d] In recent years we have developed a novel approach for organizing chromophore-electron acceptor diad assemblies (especially pseudorotaxane-type assemblies) by the application of donor-modified chromophores that form the supramolecular noncovalently linked diads with the electron acceptor via donor−acceptor $\pi-\pi$ interaction.[8e−i] Time-resolved studies have been carried out in a collaboration project with Willner.[8j−l] In this paper, we report for the first time (1) the template-directed assembly of a novel [2]catenane (**8**) incorporating a ruthenium−tris(2,2′-bipyridine) complex (sensitizer) and a cyclobis(paraquat-*p*-phenylene) (BXV^{4+}, acceptor) (Scheme 1) and (2) photoinduced intramolecular electron transfer in this catenane complex.

Scheme 1. Sequence of Reactions Leading to [2]Catenane **7** and Complex **8** (L = 4,4′-Dimethyl-2,2′-bipyridine)

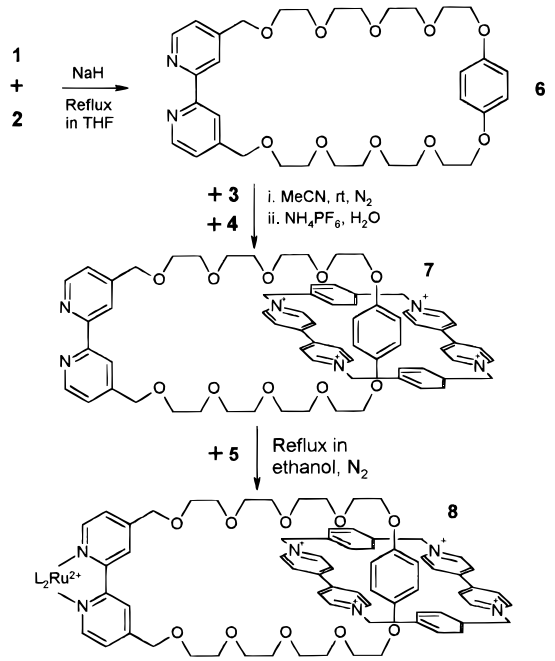

The syntheses of the catenane ligand **7** and the catenane complex **8** are shown in Scheme 1. 1,4-Bis[1-(*p*-tolylsulfonyloxy)-3,6,9-trioxaundecyloxy]benzene (**1**)[9] was reacted with 4,4′-bis(hydroxymethyl)-2,2′-bipyridine (**2**) in the presence of NaH to give the macrocyclic polyether **6** in 51% yield. Reacting the macrocyclic polyether **6** with 1,1′-[1,4-phenylenebis(methylene)]bis-4,4′-bipyridinium bis(hexafluorophosphate) (**4**) and 1,4-bis(bromomethyl)benzene (**3**) in MeCN at ambient temperature and pressure afforded the [2]catenane **7·4PF$_6$**, which was isolated as a red solid in 50% yield after column chromatography on neutral alumina (methanol-saturated methanol solution of NH_4Cl (1:1 v:v)) and counterion exchange. Reacting the chloride salt of **7** with *cis*-dichloro-bis(4,4′-dimethyl-2,2′-bipyridine)ruthenium(II) (**5**) in ethanol under reflux and N_2 atmosphere afforded the ruthenium complex **8·6Cl**. The catenane-type complex **8·6Cl** was isolated as a dark solid in 40% yield after size exclusion chromatography (Sephadex G-15, H_2O). For our study, the counterion of **8** was changed to **PF$_6$**- to increase its solubility in CH_3CN. Reference complex **9** was prepared by reacting crown ether **6** with ruthenium complex **5** under refluxing and N_2 in ethanol for 3 days. Complex **9** was obtained in 65% yield after column chromatography (silica, $CH_2Cl_2-CH_3OH$ (92:8/v:v)).

The interlocking of the two macrocycles in catenane ligand **7** and in the complex **8** was comfirmed by the X-ray crystal structure of **7**. In the single-crystal structure[10] of **7·4PF$_6$** (Figure 1), the hydroquinone ring is positioned in the cavity (inside) of the tetracationic cyclophane and the 2,2′-bipyridine component is on

(1) FB. 11.2 Organische Chemie, Universität des Saarlandes.
(2) Engler-Bunte Institut der Universität Karlsruhe.
(3) FB. 11.1 Anorganische Chemie, Universität des Saarlandes.
(4) (a) Deisenhofer, J.; Epp, O.; Miki, K.; Huber, R.; Michel, H. *J. Mol. Biol.* **1984**, *180*, 385. (b) Deisenhofer, J.; Epp, O.; Miki, K.; Huber, R.; Michel, H. *Nature* **1985**, *318*, 618. (c) Chang, C. H.; Tiede, D.; Tang, J.; Smith, U.; Norris, J.; Schiffer, M. *FEBS Lett.* **1986**, *205*, 82.
(5) (a) Moser, C. C.; Keske, J. M.; Warncke, K.; Farid, R. S.; Dutton, P. L. *Nature* **1992**, *355*, 796. (b) Pelletier, H.; Kraut, J. *Science* **1992**, *258*, 1748. (c) Beratan, D. N.; Onuchic, J. N.; Winkler, J. R.; Gray, H. B. *Science* **1992**, *258*, 1740.
(6) (a) Sessler, J. L.; Wang, B.; Harriman, A. *J. Am. Chem. Soc.* **1993**, *115*, 10418. (b) Harriman, A.; Kubo, Y.; Sessler, J. L. *J. Am. Chem. Soc.* **1992**, *114*, 388. (c) Turro, C.; Chang, C. K.; Leroi, G. E.; Cukier, R. I.; Nocera, D. G. *J. Am. Chem. Soc.* **1992**, *114*, 4013. (d) Sun, L.; von Gersdorff, J.; Niethammer, D.; Tian, P.; Kurreck, H. *Angew. Chem., Int. Ed. Engl.* **1994**, *33*, 2318. (e) Sun, L.; von Gersdorff, J.; Sobek, J.; Kurreck, H. *Tetrahedron* **1995**, *21*, 471. (f) Dürr, H.; Bossmann, S.; Kropf, M.; Hayo, R.; Turro, N. J. *J. Photochem. Photobiol. A* **1994**, *80*, 341. (g) Linke, M.; Chambron, J.-C.; Heitz, V.; Sauvage, J.-P. *J. Am. Chem. Soc.* **1997**, *119*, 11329. (h) Anelli, P. L.; Ashton, P. R.; Ballardini, R.; Balzani, V.; Gandolfi, M. T.; Goodnow, T. T.; Kaifer, A. E.; Philp, D.; Pietraszkiewicz, M.; Prodi, L.; Reddington, M. V.; Slawin, A. M. Z.; Spencer, N.; Stoddart, J. F.; Vicent, C.; Williams, D. J. *J. Am. Chem. Soc.* **1992**, *114*, 193. (i) Amabilino, D. B.; Stoddart, J. F. *Chem. Rev.* **1995**, *95*, 2725. (j) Philp, D.; Stoddart, J. F. *Angew. Chem., Int. Ed. Engl.* **1996**, *35*, 1154.
(7) (a) Carina, R. F.; Dietrich-Buchecker, C.; Sauvage, J.-P. *J. Am. Chem. Soc.* **1996**, *118*, 9110. (b) Kern, J.-M.; Sauvage, J.-P.; Weidmann, J.-L.; Mrmaroli, N.; Flamigni, L.; Ceroni, P.; Balzani, V. *J. Am. Chem. Soc.* **1997**, *36*, 55329. (c) Benniston, A. C.; Harriman, A.; Yufit, D. S. *Angew. Chem.* **1997**, *109*, 2451. (d) Benniston, A. C.; Mackie, P. R.; Harriman, A. *Angew. Chem.* **1998**, *110*, 376.
(8) (a) Bossmann, S. Ph.D. Thesis, Universität des Saarlandes, 1991. (b) Seiler, M. Ph.D. Thesis, Universität des Saarlandes, 1994. (c) Kropf, M. Ph.D. Thesis, Universität des Saarlandes, 1995. (d) David, E. Ph.D. Thesis, Universität des Saarlandes, 1997. (e) Bossmann, S.; Dürr, H. *New J. Chem.* **1992**, *16*, 769. (f) Dürr, H.; Bossmann, S.; Schwarz, R. *J. Inf. Rec. Mats.* **1994**, *21*, 471. (g) Seiler, M.; Dürr, H. *Synthesis* **1994**, 83. (h) Kropf, M.; Dürr, H.; Collet, C. *Synthesis* **1996**, 609. (i) Seiler, M.; Dürr, H. *Liebigs Ann.* **1995**, 407. (j) Seiler, M.; Dürr, H.; Willner, I.; Joselevich, E.; Doron, A.; Stoddart, J. F. *J. Am. Chem. Soc.* **1994**, *116*, 3399. (k) Kropf, M.; Joselevich, E.; Dürr, H.; Willner, I. *J. Am. Chem. Soc.* **1996**, *118*, 655. (l) David, E.; Born, R.; Kaganer, E.; Joselevich, E.; Dürr, H.; Willner, I. *J. Am. Chem. Soc.* **1997**, *119*, 7778.
(9) Marquis, D.; Greiving, H.; Desvergne, J.-P.; Lahrahar, N.; Marsau, P.; Hopf, H.; Bouas-Laurent, H. *Liebigs Ann.* **1997**, 97.

S0002-7863(98)00332-1 CCC: $15.00
Published on Web 05/30/1998

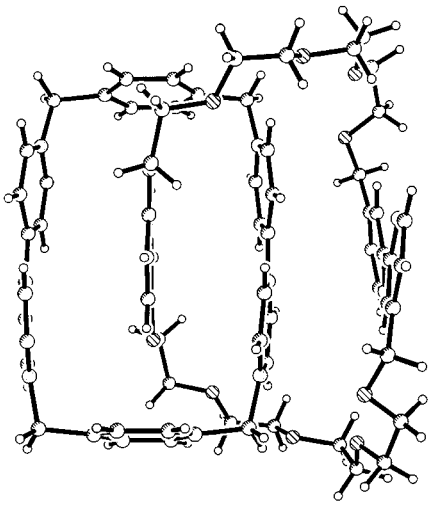

Figure 1. The crystal structure of **7·4PF6** (ball-and-stick representation).

the "outside". The molecular complex has C_2 (2) crystal point symmetry, the 2-fold axis running through three C−C bonds and the center of the $-O-C_6H_4-O-$ unit. The tilt angle of the $-OC_6H_4O-$ axis of the "inside" hydroquinone ring to the mean plane of the tetracationic cyclophane is 48°, whereas that of the outside 2,2′-bipyridine ring system is 112°. The inside hydroquinone ring, forced by symmetry, is exactly centrally located within the tetracationic cyclophane, which has a length and breadth of 10.24 Å and 6.90 Å, respectively. The mean interplanar separations between the inside hydroquinone ring and the outside and the inside bipyridinium units are 3.49 Å and 3.41 Å. The centroid−centroid separation between the outside 2,2′-bipyridine and the inside bipyridinium unit is 3.39 Å, indicating strong $\pi-\pi$ interaction between these two units. Secondary stabilization of the $\pi-\pi-\pi-\pi$ [2]catenane structure is achieved by a combination of (1) edge-to-face [C−H···π] interactions between the inside hydroquinone CH hydrogen atoms and the two *p*-xylene spacers of the tetracationic cyclophane ([H···π], 2.95 Å; [C−H···π], 164°) and (2) [C−H···O] hydrogen bonds between bipyridinium protons and the central oxygen of each polyether linkage ([C···O], 3.14 Å; [H···O], 2.24 Å; C−H···O angle, 162.5°). The 2,2′-bipyridine system adopts a trans-conformation, and the torsion angle between the two pyridine planes is −12.5°. The crystal contains two enantiomeric forms possible for **7·4PF$_6$** (Figure 1).

Electrochemical studies made with catenane **8** in deoxygenated acetonitrile showed that the metal center undergoes a reversible one-electron oxidation step corresponding to a half-wave potential of $E_{Ru2+/3+} = 1.20$ V (vs SCE). The potential difference between the peaks of the oxidation and reduction waves was $\Delta E = 64$ mV. For $Ru(bpy)_3(PF_6)_2$, ΔE was 60 mV. Upon reductive scans, two sets of redox waves characteristic with the linked tetracationic cyclophane can be observed before the appearance of the couple Ru^{2+}/Ru^{+} (−1.39 V; $\Delta E = 60$ mV). The first redox couple at −0.34 V ($\Delta E = 111$ mV) corresponds to the reduction of both paraquat units within the tetracationic cyclophane from +2 to +1 state. The second at −0.71 V ($\Delta E = 64$ mV) corresponds to the reduction of both subunits to yield the neutral molecule. The energy for the 0−0 transition (E_{0-0}) of **8** in CH_3CN was measured to be 2.16 eV (Table 1). Therefore, the thermodynamic driving force for the photoinduced electron transfer in **8** from the excited metal center to the noncovalently linked tetracationic cyclophane was calculated to be −0.62 eV, ignoring Coulombic terms (according to eq 1).[11] This indicates that the intramolecular electron transfer in **8** is thermodynamically favored.

Table 1. Absorption and Emission Properties of the Compounds Studied in Acetonitrile

compound	λ_{max} (nm) (log ϵ)	λ_{em} (nm)	ϕ_{em}	E_{0-0} (eV)
7	475 (2.85)			
8	463 (4.13)	644	0.0021	2.16
9	461 (4.11)	635	0.049	2.17

$$\Delta G = F^*[E(S^*/S^+) - E(A/A^-)] \quad (1)$$

Further evidence for the intramolecular electron transfer in catenane **8** comes from spectroscopic studies. The spectroscopic properties of **8** and the reference **9** are shown in Table 1. Both **8** and **9** absorb strongly around 462 nm, which is associated with the metal-to-ligand charge-transfer (MLCT) transitions. Nevertheless, the peak half-width of **8** (118 nm) is much broader than that of **9** (79 nm), due to the presence of the charge-transfer absorption band associated with the [2]catenane, which is clearly evident in **7** as a broad band centered around 475 nm (peak at half-width = 132 nm). Comparison of the emission spectra of **8** and **9** (**7** is nonluminescent) in N_2 saturated acetonitrile showed that, in the catenane complex (**8**), i.e., association with BXV^{4+}, the emission maximum shifted from 635 nm (**9**) to 644 nm (**8**), and the emission quantum yield was reduced from 0.049 (**9**) to 0.0021 (**8**). Measurements at different concentrations reveal that the emission quenching in **8** is intramolecular. Clearly, the marked decrease in emission quantum yield results from the intramolecular electron transfer in **8** from the excited Ru^{2+} complex (MLCT state) to BXV^{4+}. Thus, the electron-transfer rate in **8** can be roughly estimated according to eq 2:

$$k_{ET} = (1/\tau_0)(\phi_0/\phi - 1) \quad (2)$$

In this equation, ϕ and ϕ_0 are the emission quantum yield of **8** and the reference **9**, respectively, and τ_0 is the emission lifetime of **9**. With $\tau_0 = 867$ ns (obtained by single-photon-counting), the value found for k_{ET} is 2.6×10^7 s^{-1}, which is comparable to that obtained for pseudorotaxane-type Ru−tris(bipyridine)−BXV^{4+} assemblies.[8l] It is expected that association of BXV^{4+} in **8** may extend the bridging chains due to electrostatic repulsion and as a result the photogenerated redox product can be stabilized against back electron transfer. Studies with the reference complex **9** and BXV^{4+} revealed that a distinct luminescence and lifetime quenching occurred only at higher concentrations of the acceptor (**9**:BXV^{4+} > 1:100). Dynamic quenching was predominant. Thus, we conclude that the Ru^{2+}−polypyridine catenane **8** can undergo efficient intramolecular electron transfer.

Acknowledgment. This research project was supported by the Volkswagen-Stiftung, the Fonds der Chemie Industrie, and the Alexander von Humboldt Foundation (Y.Z.H.).

Supporting Information Available: Spectral data and characterization for compounds **6**−**9** and crystallographic data for **7** (9 pages, print/PDF). See any current masthead page for ordering information and Web access instructions.

JA980332S

(10) Crystal data, data collection and structure refinement for **7·4PF$_6$**: empirical formula $C_{78}H_{88}F_{24}N_{10}O_{10}P_4$, $M_r = 1905.46$, monoclinic, space group *I*2/*a*, $a = 22.059(4)$ Å, $b = 13.583(3)$ Å, $c = 29.281(6)$ Å, $\alpha = 90°$, $\beta = 91.11\ (3)°$, $\gamma = 90°$, $V = 8772(3)$ Å^3, $Z = 4$, $\rho_{calcd} = 1.443$ Mg/m^3. Crystal of size 0.4 × 0.2 × 0.18 mm. Stoe IPDS diffractometer, Image plate. Temperature 293(2) K, $\lambda = 0.710\ 73$ Å. Monochromator: graphite. Control reflections: 50 to 200 ($I > 6\sigma(I)$) on each image. θ range for data collection: 2.23 to 24.14°. The structure was solved by direct methods and refined by full-matrix least-squares on F^2; 27 253 reflections collected of which 3579 ($I > 2\sigma(I)$) were classified as observed out of 6574 unique reflection. Programs used: SHELXS-97 (Sheldrick, 1990) and SHELXL-97 (Sheldrick, 1997). Goodness-of-fit on F^2 1.313. Final *R* indices [$I > 2\sigma(I)$]: R1 = 0.0828, wR2 = 0.2132. *R* indices (all data): R1 = 0.1305, wR2 = 0.2330. Largest difference peak and hole: 0.519 and −0.302 eA^{-3}.

(11) Rehm, D.; Weller, A. *Isr. J. Chem.* **1970**, *8*, 259.